Preparation, Crystal Structure, and Thermolysis of Phenylenediammonium Diperchlorate Salts†

Inder Pal Singh Kapoor,‡ Pratibha Srivastava,‡ Gurdip Singh,*,‡ Udai P. Singh,£ and Roland Fröhlich§

Department of Chemistry, DDU Gorakhpur University, Gorakhpur-273 009, India, Department of Chemistry, Indian Institute of Technology, Roorkee, Roorkee-247 667, Uttaranchal, India, and Organisch-Chemisches Institut, Universität Münster, D-48149 Münster, Germany

Received: October 10, 2007; In Final Form: November 1, 2007

Three salts of phenylenediammonium diperchlorate have been prepared and characterized by X-ray crystallography. Their thermal decomposition has been studied by thermogravimetry (TG), differential thermal analysis (DTA), and explosion delay (D_E) measurements. The kinetics of thermal decomposition was evaluated by model fitting and isoconversional methods using TG data. The oxidation−reduction reactions near the surface of thermolysing perchlorates may be responsible for the decomposition followed by explosion. The possible pathways of thermolysis have also been proposed.

Introduction

All of the perchlorates find application in explosives and propellants. Ammonium perchlorate (AP)[1,2] can be regarded as the most important perchlorate salt which is used as an oxidizer in the composite solid propellants. Studies of the thermolysis of substituted ammonium perchlorates[3,4] and diammonium perchlorates[5−8] have already been reported. These compounds have been reported to sublimate and decompose at lower temperatures and explode readily at higher temperature. These are generally more violent in their explosive behavior as compared to nitrate salts.[9−12]

Singh et al.[13−17] have prepared and characterized a large number of ring-substituted arylammonium perchlorates. The proton-transfer process has been proposed as the rate determining step. It seems that an oxidative−reductive reaction between arylamine and $HClO_4$ and/or its decomposition products causes explosion. Very recently, we have prepared, characterized, and investigated the thermolysis of phenylenediammonium dinitrate salts.[18]

In the light of the above findings, we decided to undertake a systematic investigation of the phenylenediammonium diperchlorate (PDADP) salts. Their preparation, crystal structure, and thermal and explosive characteristics are discussed in the present article.

Experimental Section

Materials. All commercially available chemicals of AR grade, such as phenylene-1,2-diamine (s.d.fine), phenylene-1,4-diamine (Alfa Aesar), and 5-carboxyl-1,3-phenylenediamine (Merck) were purified from distilled water. The 70% perchloric acid (Merck) silica gel TLC grade (Ranbaxy), iodine (s.d.fine), and nitron (Loba) were used as received.

Preparation and Characterization. Diperchlorates (**Caution!** PDADPs are explosion hazards) were prepared at room temperature by reacting cold 20% aqueous perchloric acid with the corresponding phenylenediamine (PDA) directly in a 1:2 molar ratio in accordance with the reaction

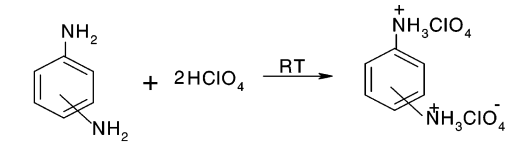

Ortho and para

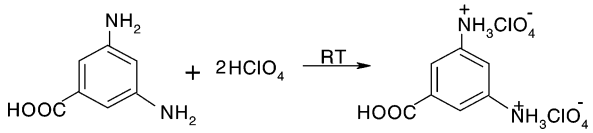

Ortho, para, and carboxylic diperchlorates were crystallized out immediately. Meta phenylenediamine salt could not be precipitated out under these conditions. The reason is still uncertain. All of these colored perchlorates were recrystallized from aqueous solution in good yield (64−82%), and their purity was checked by thin-layer chromatography (TLC). Moreover, these salts were characterized by IR (Perkin-Elmer RXI spectrometer), a gravimetric method using Nitron reagent,[19] and X-ray crystallography. The crystal parameters are shown in Tables 1−3 and physical parameters, TLC, and IR data in Table 4.

Crystallographic Study. Crystals of all three PDADP salts were obtained by recrystallization from the aqueous solution. The data collection on the crystal of P-1,2-DADP was performed at low temperature (198 K) using a Nonius Kappa CCD diffractometer equipped with a rotatory anode generator Nonius FR 591. The programs that were used involved data collection by Collect (Nonius B.V.1998)[20] and data reduction by Denzo-SMN (Otwinowski and Minor, 1997).[21] The structure was solved by direct methods (program SHELXS-97)[22] and refined by the full matrix least-squares method on all F^2 data using SHELXL-

* To whom correspondence should be addressed. E-mail: gsingh4us@yahoo.com. Phone: 91-551-2200745 (R) 2202856 (O). Fax: 91-551-2340459.

† Part 53.

‡ DDU Gorakhpur University.

£ Indian Institute of Technology.

§ Universität Münster.

10.1021/jp709875b CCC: $40.75
Published on Web 01/09/2008

TABLE 1: Crystal Data and Structure Refinement for PDADP

salts designation	P-1,2-DADP	P-1,4-DADP	5-carboxyl-P-1,3-DADP
empirical formula	$C_6H_{12}Cl_2N_2O_9$	$C_6H_{10}Cl_2N_2O_8$	$C_7H_{14}Cl_2N_2O_{12}$
formula weight	327.08	309.06	389.10
temp/K	223(2) K	100 K	100 K
λ/Å	0.71073 Å	0.71073 Å	0.71073 Å
crystal system	triclinic, $P\bar{1}$ (No. 2)	triclinic ($P1$)	monoclinic (Cc)
cell constants	$a = 7.404(1)$ Å $\alpha = 72.60(1)°$.	$a = 5.0970(8)$ $\alpha = 103.625(9)$	$a = 9.2503(4)$ $\alpha = 90.00$
	$b = 8.105(1)$ Å $\beta = 73.29(1)°$	$b = 7.1061(13)$ $\beta = 103.274(9)$	$b = 23.4730(9)$ $\beta = 109.718(2)$
	$c = 11.790(1)$ Å $\gamma = 63.11(1)°$	$c = 8.7475(12)$ $\gamma = 108.086(9)$	$c = 7.1360(3)$ $\gamma = 90.00$
volume	592.42(12) Å^3	276.54(8) Å^3	1458.60(11) Å^3
molecules per unit cell, Z	2, 1.834 Mg/m^3	1, 1.856 mg/m^3	4, 1.772 mg/m^3
absorption coefficient	0.596 mm^{-1}	0.626 mm^{-1}	0.514 mm^{-1}
$F(000)$	336	158	800
crystal size/nm	0.40 × 0.30 × 0.25 mm	0.34 × 0.25 × 0.18	0.35 × 0.28 × 0.20
q range for data collection	1.84−27.82°	2.54−34.99	1.74−46.98
limiting indices	$-8<=h<=9$	$-8<=h<=8$	$-19<=h<=19$
	$-10<=k<=10$	$-11<=k<=11$	$-48<=k<=30$
	$-15<=l<=15$	$-14<=l<=14$	$-14<=l<=13$
reflections collected/unique	5325/2764 [R(int) = 0.0488]	2426/2176 [R(int) = 0.0562]	6664/6075 [R(int)= 0.0279]
data/restraints/parameters	2764/0/182	2426/3/165	6664/0/217
goodness-off-fit on F^2	1.004	1.206	0.974
final R indices [$I > 2\sigma(I)$]	R1 = 0.0454, wR2 = 0.1261	R1 = 0.0849, wR2 = 0.2133	R1 = 0.0339, wR2 0.0970
R indices (all data)	R1 = 0.0540, wR2 = 0.1321	R1 = 0.0986, wR2 = 0.2214	R1 = 0.0415, wR2 = 0.1057
refinement method	full matrix least-squares on F^2	full matrix least-squares on F^2	full matrix least-squares on F^2
CCDC No.	660980	661734	661733

TABLE 2: Bond Length (Å) Data for PDADP

P-1,2-DADP		P-1,4-DADP		5-carboxyl-P-1,3-DADP	
C(1)−C(6)	1.381(3)	C1 C2	1.329(15)	C1 C6	1.3847(11)
C(1)−C(2)	1.383(3)	C1 C6	1.489(13)	C1 C2	1.3886(11)
C(1)−N(1)	1.467(3)	C1 H1	0.9300	C1 H1	0.9300
N(1)−H(1A)	0.9000	C2 C3	1.381(13)	C2 C3	1.3830(11)
N(1)−H(1B)	0.9000	C2 H2	0.9300	C3 C4	1.3972(11)
N(1)−H(1C)	0.9000	C3 C4	1.348(10)	C3 H3	0.9300
C(2)−C(3)	1.380(4)	C4 C5	1.421(10)	C4 C5	1.3949(11)
C(2)−N(2)	1.468(3)	C4 H4	0.9300	C4 C7	1.4867(11)
N(2)−H(2A)	0.9000	C5 C6	1.393(10)	C5 C6	1.3861(11)
N(2)−H(2B)	0.9000	C5 H5	0.9300	C5 H5	0.9300
N(2)−H(2C)	0.9000	N1 C6	1.440(10)	N1 C6	1.4559(11)
C(3)−C(4)	1.391(4)	N1 H1A	0.8900	N1 H1A	0.8900
C(3)−H(3)	0.9400	N1 H1B	0.8900	N1 H1B	0.8900
C(4)−C(5)	1.371(4)	N1 H1C	0.8900	N1 H1C	0.8900
C(4)−H(4)	0.9400	N2 C3	1.478(11)	N2 C2	1.4586(10)
C(5)−C(6)	1.384(4)	N2 H2A	0.8900	N2 H2A	0.8900
C(5)−H(5)	0.9400	N2 H2B	0.8900	N2 H2B	0.8900
C(6)−H(6)	0.9400	N2 H2C	0.8900	N2 H2C	0.8900
Cl(1)−O(11)	1.421(2)	Cl1 O4	1.421(8)	Cl1 O6	1.4284(9)
Cl(1)−O(12)	1.424(2)	Cl1 O2	1.426(8)	Cl1 O5	1.4322(8)
Cl(1)−O(14)	1.432(2)	Cl1 O3	1.439(6)	Cl1 O4	1.4565(8)
Cl(1)−O(13)	1.437(2)	Cl1 O1	1.484(7)	Cl1 O3	1.4579(7)
Cl(2)−O(21)	1.418(2)	Cl2 O8	1.405(7)	Cl2 O10	1.4380(10)
Cl(2)−O(22)	1.435(2)	Cl2 O6	1.427(7)	Cl2 O9	1.4464(8)
Cl(2)−O(23)	1.446(2)	Cl2 O5	1.439(5)	Cl2 O7	1.4474(8)
Cl(2)−O(24)	1.4471(19)	Cl2 O7	1.465(6)	Cl2 O8	1.4491(8)
O(1)−H(11)	0.91(6)			O1 C7	1.2192(12)
O(1)−H(12)	0.75(7)			O2 C7	1.3224(12)
				O2 H2	0.8200
				O12 H21	0.83(3)
				O12 H22	0.76(4)
				O15 H19	0.80(4)
				O15 H20	0.71(3)

97 (Sheldrick, 1997).[23] The X-ray data collection and processing for P-1,4-DADP and 5-carboxyl-P-1,3-DADP were performed on Bruker Kappa Apex four circle CCD detector with graphite-monochromated Mo Kα radiation ($\lambda = 0.71070$ Å) at 100 (±2) K. Crystal structures were solved by direct methods. Structure solution, refinement, and data output were carried out with the SHELXTL program.[22,23] Hydrogen atoms were placed in geometrically calculated positions by using a riding model. Images were created with the DIAMOND program.[24] Refinement with anisotropic thermal parameters for non-hydrogen atoms led to R values of 0.045, 0.084, and 0.033 respectively for P-1,2-DADP, P-1,4-DADP, and 5-carboxyl-P-1,3-DADP. The crystal structures of these salts are shown in Figures 1−3, while crystal parameters, bond lengths, and bond angle data are summarized in Tables 1−3.

Thermal Decomposition of PDADP. *Non-isothermal Thermogravimetry (TG) and Differential Thermal Analysis (DTA) in Static Air*. Non-isothermal TG studies on the salts (wt ∼ 33 mg, 100−200 mesh) were undertaken in static air at the heating rate of 10 ± 1 °C min^{-1} using an indigenously fabricated TG apparatus.[25] A round-bottom platinum crucible was used as the sample holder. The fractional decomposition (α) has been plotted against temperature (°C), and the thermograms are shown in Figure 4. DTA curves of these salts (Figure 5) were obtained on the Universal Thermal Analysis Instrument, Mumbai, at 10 °C min^{-1} in flowing air (60 mL min^{-1}) using 20 mg of sample. The TG and DTA phenomenological data are summarized in Table 5.

Isothermal TG. The isothermal TGs (33 mg, 100−200 mesh) were taken in static air using the above-said TG apparatus at appropriate temperatures. The fractional decomposition (α) has been plotted against time (min), and the thermograms are shown in Figure 6.

Explosion Delay Measurements. The explosion delay (D_E) measurements were undertaken using the tube furnace technique[26] in the temperature range of 300−405 °C (±1 °C). Each run was repeated three times, and mean values are reported in Table 6. The D_E data were found to fit in the following equation[27−30]

$$D_E = A \exp(E_a^*/RT) \quad (1)$$

where E_a* is the activation energy for thermal explosion, A the pre-exponential factor, and T the absolute temperature. E_a*'s assessed by eq 1 along with the correlation coefficients (r) are given in Table 6.

Percent Oxygen Balance and Velocity of Detonation. The percent oxygen balance (OB) was calculated by the equation of Martin and Yallop[31]

$$OB = [(z - 2x - y/2)100]/n \quad (2)$$

TABLE 3: Bond Angle (°) Data for PDADP

P-1,2-DADP		P-1,4-DADP		5-carboxyl-P-1,3-DADP	
C(6)−C(1)−C(2)	119.9(2)	C2 C1 C6	119.3(9)	C6 C1 C2	118.18(7)
C(6)−C(1)−N(1)	117.9(2)	C2 C1 H1	120.4	C6 C1 H1	120.9
C(2)−C(1)−N(1)	122.1(2)	C6 C1 H1	120.4	C2 C1 H1	120.9
C(1)−N(1)−H(1A)	109.5	C1 C2 C3	119.4(9)	C3 C2 C1	121.83(7)
C(1)−N(1)−H(1B)	109.5	C1 C2 H2	120.3	C3 C2 N2	120.79(7)
H(1A)−N(1)−H(1B)	109.5	C3 C2 H2	120.3	C1 C2 N2	117.37(7)
C(1)−N(1)−H(1C)	109.5	C4 C3 C2	124.9(6)	C2 C3 C4	118.51(7)
H(1A)−N(1)−H(1C)	109.5	C4 C3 N2	116.9(8)	C2 C3 H3	120.7
H(1B)−N(1)−H(1C)	109.5	C2 C3 N2	118.2(7)	C4 C3 H3	120.7
C(3)−C(2)−C(1)	120.4(2)	C3 C4 C5	118.4(7)	C5 C4 C3	121.10(7)
C(3)−C(2)−N(2)	118.4(2)	C3 C4 H4	120.8	C5 C4 C7	120.13(7)
C(1)−C(2)−N(2)	121.2(2)	C5 C4 H4	120.8	C3 C4 C7	118.75(7)
C(2)−N(2)−H(2A)	109.5	C6 C5 C4	119.0(7)	C6 C5 C4	118.22(7)
C(2)−N(2)−H(2B)	109.5	C6 C5 H5	120.5	C6 C5 H5	120.9
H(2A)−N(2)−H(2B)	109.5	C4 C5 H5	120.5	C4 C5 H5	120.9
C(2)−N(2)−H(2C)	109.5	C5 C6 N1	121.4(7)	C1 C6 C5	122.13(7)
H(2A)−N(2)−H(2C)	109.5	C5 C6 C1	119.0(7)	C1 C6 N1	119.36(7)
H(2B)−N(2)−H(2C)	109.5	N1 C6 C1	119.5(7)	C5 C6 N1	118.51(7)
C(2)−C(3)−C(4)	119.5(2)	C6 N1 H1A	109.5	C6 N1 H1A	109.5
C(2)−C(3)−H(3)	120.2	C6 N1 H1B	109.5	C6 N1 H1B	109.5
C(4)−C(3)−H(3)	120.2	H1A N1 H1B	109.5	H1A N1 H1B	109.5
C(5)−C(4)−C(3)	119.9(3)	C6 N1 H1C	109.5	C6 N1 H1C	109.5
C(5)−C(4)−H(4)	120.0	H1A N1 H1C	109.5	H1A N1 H1C	109.5
C(3)−C(4)−H(4)	120.0	H1B N1 H1C	109.5	H1B N1 H1C	109.5
C(4)−C(5)−C(6)	120.6(2)	C3 N2 H2A	109.5	C2 N2 H2A	109.5
C(4)−C(5)−H(5)	119.7	C3 N2 H2B	109.5	C2 N2 H2B	109.5
C(6)−C(5)−H(5)	119.7	H2A N2 H2B	109.5	H2A N2 H2B	109.5
C(1)−C(6)−C(5)	119.6(2)	C3 N2 H2C	109.5	C2 N2 H2C	109.5
C(1)−C(6)−H(6)	120.2	H2A N2 H2C	109.5	H2A N2 H2C	109.5
C(5)−C(6)−H(6)	120.2	H2B N2 H2C	109.5	H2B N2 H2C	109.5
O(11)−Cl(1)−O(12)	109.77(17)	O4 Cl1 O2	110.4(5)	O6 Cl1 O5	110.87(7)
O(11)−Cl(1)−O(14)	108.88(15)	O4 Cl1 O3	109.6(5)	O6 Cl1 O4	109.56(7)
O(12)−Cl(1)−O(14)	108.99(16)	O2 Cl1 O3	112.2(5)	O5 Cl1 O4	109.44(6)
O(11)−Cl(1)−O(13)	110.56(15)	O4 Cl1 O1	107.8(4)	O6 Cl1 O3	110.03(5)
O(12)−Cl(1)−O(13)	108.85(15)	O2 Cl1 O1	110.2(5)	O5 Cl1 O3	109.31(5)
O(14)−Cl(1)−O(13)	109.76(13)	O3 Cl1 O1	106.6(4)	O4 Cl1 O3	107.56(5)
O(21)−Cl(2)−O(22)	110.83(15)	O8 Cl2 O6	113.0(5)	O10 Cl2 O9	109.90(6)
O(21)−Cl(2)−O(23)	109.75(14)	O8 Cl2 O5	110.2(4)	O10 Cl2 O7	109.71(5)
O(22)−Cl(2)−O(23)	108.71(13)	O6 Cl2 O5	109.7(4)	O9 Cl2 O7	109.43(5)
O(21)−Cl(2)−O(24)	110.06(13)	O8 Cl2 O7	106.6(4)	O10 Cl2 O8	110.09(6)
O(22)−Cl(2)−O(24)	109.89(13)	O6 Cl2 O7	106.4(4)	O9 Cl2 O8	108.87(5)
O(23)−Cl(2)−O(24)	107.54(12)	O5 Cl2 O7	110.8(4)	O7 Cl2 O8	108.82(5)
H(11)−O(1)−H(12)	100(6)			C7 O2 H2	109.5
				O1 C7 O2	124.13(8)
				O1 C7 C4	122.83(8)
				O2 C7 C4	113.03(8)
				H21 O12 H22	99(3)
				H19 O15 H20	114(4)

TABLE 4: Physical Parameters, TLC, and Analytical and IR Data on PDADP

Compound	Mol. Wt.	Structural formula	Crystal colour	m.p./ °C	TLC Eluent	TLC Spot colour	R_f	Yield %	% of ClO_4^- Exp.	% of ClO_4^- Theo.	IR Frequencies
P-1,2-DADP	309		Light brown crystals	105	a:b:c 8:4:3	Yellow	0.93	82	58.91	60.85	N-H str. 3447, N-H bend 1543, C-H str.2962, C-H bend 1463, Cl=O 1315, Cl-O 1089, ClO_4^- 625
P-1,4-DADP	309		Dark purple crystals	117	a:b:c 8:4:3	Brown	0.65	76	63.55	64.40	N-H str. 3487, N-H bend 1574, C-H str.2852, C-H bend 1462, Cl=O 1309, Cl-O 1086, ClO_4^- 627
5-Carboxyl-P-1,3-DADP	353	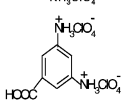	Dark brown crystals	84	a:b:c 7:5:3	Reddish	0.91	64	53.58	56.37	N-H str. 3454, N-H bend 1575, C-H str.2941, C-H bend 1462, Cl=O 1313, Cl-O 1091, ClO_4^- 626

a:b:c = water: DMSO: methanol, Locating reagent- Iodine

where *x*, *y*, and *z* are the respective number of atoms of C, H, and N, respectively, and *n* is the total number of atoms in the molecule. Furthermore, the velocity of detonation (VOD) was calculated by using the Rothstein method.[32] OB and VOD data are reported in Table 6.

Kinetic Analysis of Isothermal TG Data. Kinetic analysis of solid-state decomposition is usually based on a single-step kinetic eq 3[33]

$$d\alpha/dt = k(T)f(\alpha) \quad (3)$$

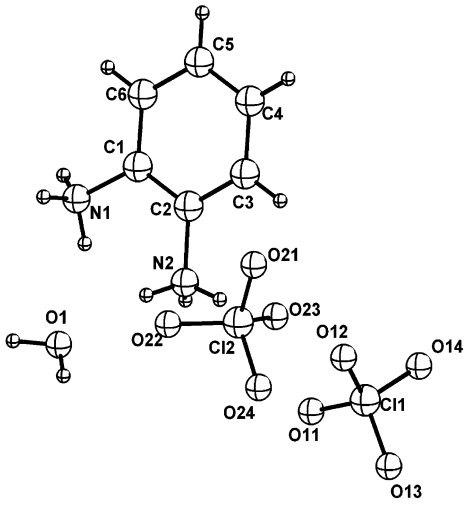

Figure 1. Crystal structure of P-1,2-DADP.

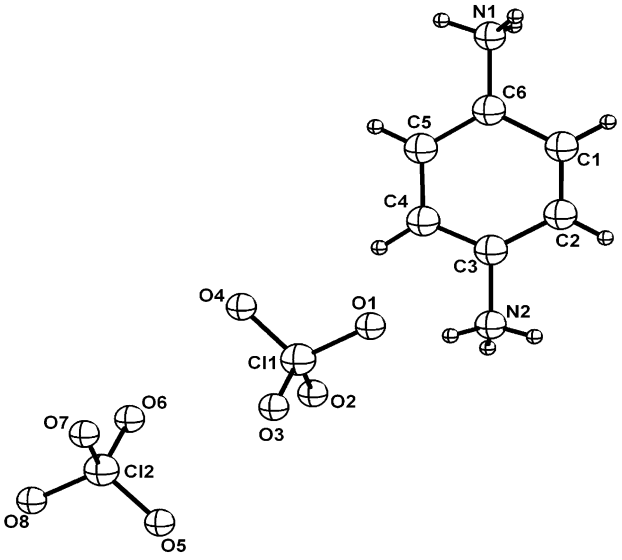

Figure 2. Crystal structure of P-1,4-DADP.

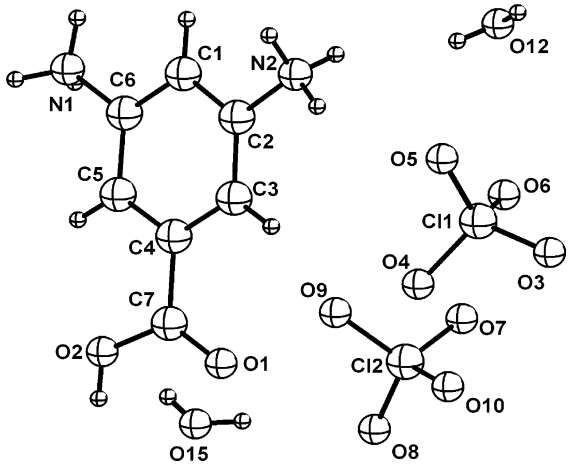

Figure 3. Crystal structure of 5-carboxyl-P-1,3-DADP.

where t is the time, T is the temperature, α is the extent of conversion ($0 < \alpha < 1$), $k(T)$ is the rate constant, and $f(\alpha)$ is the reaction model,[33] which describes the dependence of the reaction rate on the extent of reactions. The value of α is experimentally derived from the global mass loss in TG experiments. The reaction model may take various forms. The

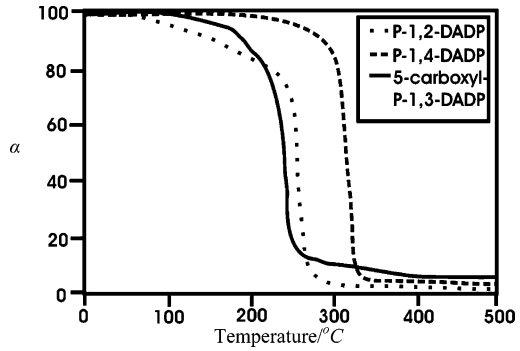

Figure 4. Non-isothermal TG of PDADP in air at standard atmospheric conditions.

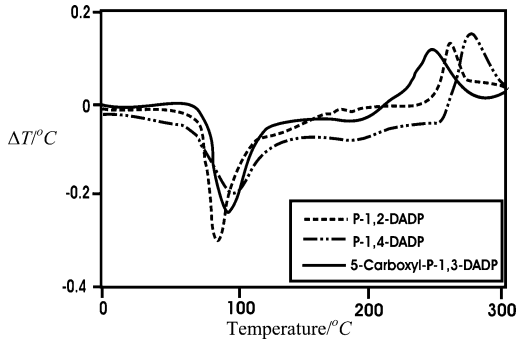

Figure 5. DTA thermogram of PDADP in air at standard atmospheric conditions.

TABLE 5: TG and DTA Phenomenological Data of PDADP in an Air Atmosphere[a]

	TG in static air			DTA peak temp. /°C	
compound	T_i/°C	T_f/°C	α	endo.	exo.
P-1,2-DADP	58	265	97	90	250
P-1,4-DADP	145	340	95	105	276
5-carboxyl-P-1,3-DADP	105	252	92	98	250

[a] T_i: initial temperature; T_f: final temperature; α: percent decomposition.

temperature dependence of $k(T)$ can be satisfactorily described by the Arrhenius equation, whose substitution into eq 3 yields

$$d\alpha/dt = A \exp(-E_a/RT)\cdot f(\alpha) \quad (4)$$

where A is a pre-exponential factor, E_a is the activation energy, and R is the gas constant.

Model Fitting Method. Rearrangement and integration of eq 3 for isothermal conditions gives

$$g_j(\alpha) = k_j(T)t \quad (5)$$

where

$$g(\alpha) = \int_0^\alpha [f(\alpha)]^{-1} d\alpha$$

is the integrated form of the reaction model. The subscript j has been introduced to emphasize that substituting a particular reaction model into eq 5 results in evaluating the corresponding rate constant which is determined from the slope of a plot of $g_j(\alpha)$ verses t. For each reaction model selected, the rate constants are evaluated at several temperatures T_i, and Arrhenius parameters are determined using the Arrhenius eq 6 in its logarithmic form

$$\ln k_j(T_i) = \ln A_j - E_j/RT_i \quad (6)$$

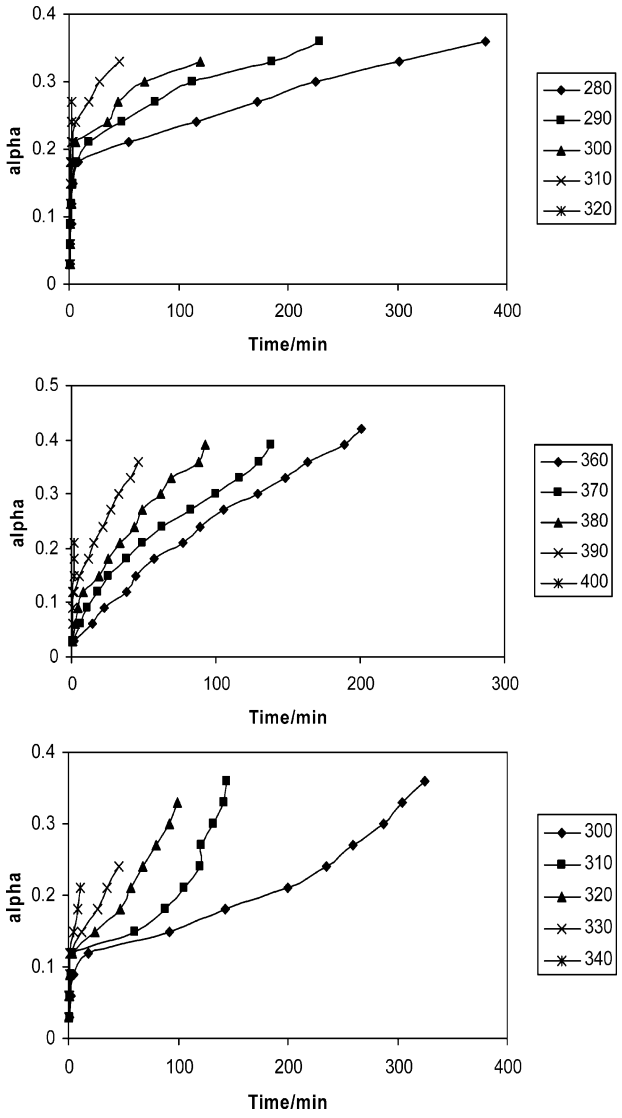

Figure 6. Isothermal TG of PDADP.

Arrhenius parameters were evaluated for isothermal experimental data by the model fitting method.

Isoconversional Method. This method allows the activation energy to be evaluated without making any assumptions about the reaction model. Additionally, the method evaluates the effective activation energy as a function of the extent of conversion which allows one to explore multistep kinetics.

The basic assumption of the isoconversional method[34] is that the reaction model as defined in eq 3 is not dependent on the temperature or heating rate. Under isothermal conditions, upon combining eq 5 and 6, we get

$$-\ln t_{\alpha,i} = \ln[A_\alpha/g(\alpha)] - E_a/RT_i \quad (7)$$

where E_a is evaluated from the slope of the plot (Figure 6) of $-\ln t_{\alpha,i}$ against T_i^{-1}. Thus, E_a's at various α's for diperchlorates have been evaluated.

Results and Discussion

The molecular structure and atom labelling scheme for PDADP are shown in Figures 1−3. The crystal parameters, bond distances, and angles are given in Tables 1−3. P-1,2-DADP and 5-carboxyl-P-1,3-DADP have, respectively, one and two H_2O molecules in their crystal lattices, but there is no H_2O of crystallization in the lattice of P-1,4-DADP. In P-1,2-DADP, the water molecule is located in between two $-^+NH_3$ moieties, whereas 5-carboxyl-P-1,3-DADP has one water positioned in between a carboxyl group and a ClO_4^- ion, and second water molecule is in between an $-^+NH_3$ moiety and another ClO_4^- ion. P-1,2-DADP crystallizes in triclinic $P\bar{1}$ with unit cell dimensions of $a = 7.404$ (1) Å, $\alpha = 72.60$ (1)°, $b = 8.105$ (1) Å, $\beta = 73.29$ (1)°, $c = 11.79(1)$ Å, and $\gamma = 63.11(1)$°; P-1,4-DADP crystallizes in triclinic $P\bar{1}$ with unit cell dimensions of $a = 5.097(8)$ Å, $\alpha = 103.62$ (9)°, $b = 7.106$ (13) Å, $\beta = 103.27$ (9)°, $c = 8.747(12)$ Å, and $\gamma = 108.08(9)$°, and 5-carboxyl-P-1,3-DADP crystallizes in monoclinic (*Cc*) with unit cell dimensions of $a = 9.250$ (4) Å, $\alpha = 90.00$°, $b = 23.473$ (9) Å, $\beta = 109.72$ (2)°, $c = 7.136(3)$ Å, and $\gamma = 90.00$° (Table 2). There are no networks of N−H···O contacts to lattice packing (Table 3) for any perchlorate. However, Brill et al.[9] have reported intramolecular hydrogen bonding in the crystal lattice of aliphatic diammonium diperchlorates. The weakness and diversity of H bonding reflect the delocalization of charge in ClO_4^- ions.

Most of the IR vibrational modes of the three PDADP salts have been assigned following previous studies of aromatic sulfates,[35−39] nitrates,[18,40−42] and perchlorates.[13−17] The frequencies and assignment are compiled in Table 4. The N−H asymmetric stretch of salts shows intense absorption in the 3447−3487 cm^{-1} range, N−H bending between 1543 and 1575 cm^{-1}, a C−H stretch between 2852 and 2962 cm^{-1}, and C−H bending in the range of 1462−1463 cm^{-1}. There is also evidence of the asymmetric stretch (broad mode) at 625−627 cm^{-1}.

Figure 4 shows the weight loss curves for PDADP salts and clearly indicates that each sample explodes during TG, P-1,2-DADP at 256 °C, P-1,4-DADP at 325 °C, and 5-carboxyl-P-1,3-DADP at 248 °C. A very thin layer of sublimate collects on the sides of the TG crucible for each salt. DTA curves (Figure 5) of each diperchlorate show that an endotherm may be due to melting/phase transformation, while an exotherm is due to the oxidation−reduction leading to explosion. A peculiar behavior of P-1,4-DADP is that it solidifies from the melt as a grayish amorphous state and then slowly crystallizes.

The kinetics of the thermal decomposition of PDADP was evaluated using 14 mechanism-based kinetic models. In the model fitting method, the kinetics is analyzed by choosing a "best-fit" model based on the value of the correlation coefficient *r* close to 1. Among various values of *r* calculated for different models, the highest value of *r* for the ortho and para isomers corresponds to model 11, while for the carboxyl derivative, it is model 1.The corresponding values of E_a as reported in Table 8 for the ortho, para, and carboxylic derivative are, respectively, 310.9, 238.3, and 208.8 kJ·mol^{-1}. A plot (Figure 7) of all of the values of the activation energy against the respective ln *A* values obtained from different models for each salt (Table 8) indicates that all of these values fall in an almost straight line, showing the existence of a kinetic compensation effect.[43,44] The kinetic compensation effect refers to the fact that under a variety of conditions, an approximately linear relationship exists between the pre-exponential factor, ln *A*, and the apparent activation energy, E_a, which are determined for a process from the Arrhenius eq 8[45]

$$\ln k = \ln A - E_a/RT \quad (8)$$

When ln *A* and E_a are linearly related, the compensation parameters *a* and *b* are defined by eq 9 for all measurements

$$\ln A = aE_a + b \quad (9)$$

TABLE 6: Explosion Delay (D_E), Activation Energy for Thermal Explosion (E_a*), Oxygen Balance (OB), and Velocity of Detonation for PDADP

		D_E/s at temp. /°C											
compound	mass mg	300 ± 1	315 ± 1	330 ± 1	345 ± 1	360 ± 1	375 ± 1	390 ± 1	405 ± 1	E_a* kJ·mol^{-1}	r	OB	VOD (mm·μs^{-1})
P-1,2-DADP	20	185	142	108	99	75	60	49	28	52.51	0.9793	−51.61	5.45
P-1,4-DADP	20	DNE[a]	DNE	DNE	195	139	101	86	71	58.35	0.9909	−53.57	4.89
5-carboxyl-P-1,3-DADP	20	70	39	26	20	19	16	13	12	50.31	0.9575	−54.84	5.09

[a] DNE: did not explode.

TABLE 7: Reaction Models Applied to Describe the Thermal Decomposition of Solids

model no.	reaction model	$f(\alpha)$	$g(\alpha)$
1	power law	$4\alpha^{3/4}$	$\alpha^{1/4}$
2	power law	$3\alpha^{2/3}$	$\alpha^{1/3}$
3	power law	$2\alpha^{1/2}$	$\alpha^{1/2}$
4	power law	$(2/3)\alpha^{-1/2}$	$\alpha^{3/2}$
5	one-dimensional diffusion	$(1/2)\alpha^{-1}$	α^2
6	Mampel (first order)	$1-\alpha$	$-\ln(1-\alpha)$
7	Avrami−Erofeev	$4(1-\alpha)[-\ln(1-\alpha)]^{3/4}$	$[-\ln(1-\alpha)]^{1/4}$
8	Avrami−Erofeev	$3(1-\alpha)[-\ln(1-\alpha)]^{2/3}$	$[-\ln(1-\alpha)]^{1/3}$
9	Avrami−Erofeev	$2(1-\alpha)[-\ln(1-\alpha)]^{1/2}$	$[-\ln(1-\alpha)]^{1/2}$
10	contracting sphere	$3(1-\alpha)^{2/3}$	$1-(1-\alpha)^{1/3}$
11	three-dimensional diffusion	$2(1-\alpha)^{2/3}[1-(1-\alpha)^{1/3}]^{-1}$	$[1-(1-\alpha)^{1/3}]^2$
12	contracting cylinder	$2(1-\alpha)^{1/2}$	$1-(1-\alpha)^{1/2}$
13	Prout−Tomkins	$\alpha(1-\alpha)$	$\ln(\alpha/1-\alpha)$
14	Ginstling−Brounshtein	$(3/2)[(1-\alpha)^{-1/3}-1]^{-1}$	$[1-(2\alpha/3)]-(1-\alpha)^{2/3}$

TABLE 8: Arrhenius Parameters for the Isothermal Decomposition of PDADP

	P-1,2-DADP			P-1,4-DADP			5-carboxyl-P-1,3-DADP		
model[a]	E_a (kJ·mol^{-1})	$-\ln A$	r	E_a (kJ·mol^{-1})	$-\ln A$	r	E_a (kJ·mol^{-1})	$-\ln A$	r
1	333.2	64.3	0.9008	324.3	60.8	0.8399	208.8	36.5	0.9697
2	355.0	66.5	0.9018	320.9	60.2	0.8408	206.7	36.2	0.9696
3	351.1	65.8	0.9033	314.2	58.9	0.8427	202.4	35.4	0.9693
4	327.8	60.5	0.9117	271.2	49.6	0.8540	173.3	28.7	0.9641
5	316.7	57.7	0.9155	249.3	44.6	0.8600	157.3	24.9	0.9579
6	333.9	62.4	0.9091	283.4	52.7	0.8491	181.8	31.2	0.9658
7	354.0	66.3	0.9020	319.5	59.9	0.8405	205.6	36.0	0.9693
8	351.8	66.0	0.9028	315.7	59.3	0.8414	203.2	35.6	0.9691
9	347.3	65.2	0.9044	307.9	57.8	0.8434	198.2	34.7	0.9686
10	335.7	61.6	0.9086	286.7	52.2	0.8484	184.1	30.5	0.9664
11	310.9	54.6	0.9170	238.3	40.4	0.8609	149.1	21.3	0.9525
12	336.6	62.1	0.9083	288.3	52.9	0.8487	185.2	31.1	0.9667
13	358.4	69.2	0.9003	327.0	63.4	0.8381	210.3	38.9	0.9694
14	312.9	55	0.9165	242.1	41.1	0.8606	151.9	21.8	0.9545

[a] Enumeration of the model is as given in Table 7.

In effect, an increase in E_a does not cause the expected decrease in the reaction rate because A increases to compensate for E_a. Equations 8 and 9 are closely related;[44] as E_a increases, an offsetting increase in ΔS^* occurs

$$\Delta G^* = E_a - T\Delta S^* \tag{10}$$

Although the physical and chemical meanings of Arrhenius parameters for heterogeneous processes are uncertain,[46] the origin of the discrepancies and validity of individual data sets can be assessed by the compensation effect as a single, general, chemical phenomenon.

The isoconversional method is known to permit estimation of the apparent activation energy independent of the model, corresponding to the extent of conversion of the sample. According to Figure 8, for a particular salt, each activation energy has a separate value at different α's. It is true[47] that energetic materials appear to have reaction characteristics that are generally consistent with the isoconversional principle as

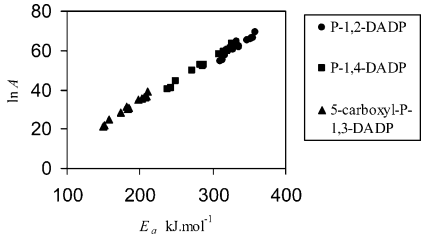

Figure 7. Variation of ln A with E_a.

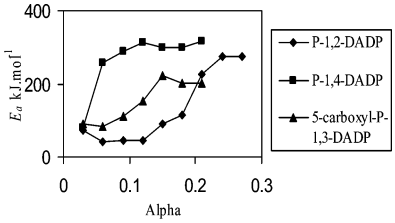

Figure 8. Dependence of the activation energy (E_a) on the extent of conversion (α) for the PDADP.

SCHEME 1

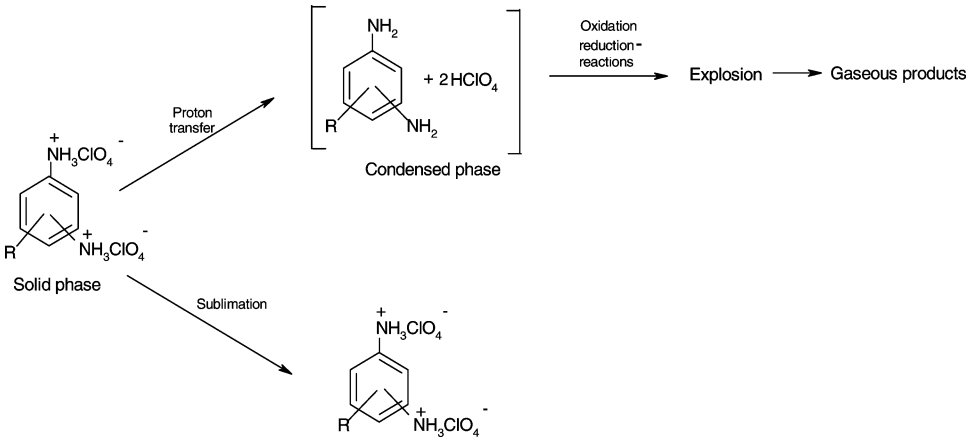

long as the confinement conditions are constant and appropriate to the intended application.

The explosion delay and activation energy for explosion in the temperature range of 300−405 °C are reported in Table 6. The energies of activation for explosion (E_a*) are, in decreasing order, P-1,4-DADP > P-1,2-DADP > 5-carboxyl-P-1,3-DADP. Among the three PDADP salts, the lowest value of E_a* for the carboxyl derivative could be due to the weakening of the N−H bond by the −I effect of the $-CO_2H$ group which facilitates proton transfer. Moreover, the lower value of E_a* for P-1,2-DADP compared to that of P-1,4-DADP is due to steric hindrance, which again, no doubt, enhances the weakening of the N−H bond. Activation energies, calculated under different temperature ranges, for isothermal kinetics and explosion delay measurements are different. The thermal decomposition process of energetic materials often involves a concert of bond-breaking and bond-forming steps under condensed or gas-phase reactions. The weakening of a particular bond seems to enhance the tendency to have a predominant, identified path to decomposition.

It seems that the overall decomposition process (Scheme 1) takes place by the transfer of a proton (N−H bond cleavage) from the arylammonium ion to ClO_4^- to form the corresponding amine and the $HClO_4$ molecule in the condensed phase prior to explosion. In fact, the gas-phase basicity of the parent amine qualitatively correlates with the tendency to liberate $HClO_4$.[46] The tendency to liberate $HClO_4$(g) decreases as the amine basicity increases. $HClO_4$ then engages in oxidation−reduction with the phenylenediamine to form gaseous products. In all three salts, some of the $HClO_4$(g) may be consumed by reaction with NH_3(g) to produce intermediate NH_4ClO_4 (not identified). Combination of NH_3 with HNO_3 to form intermediate NH_4NO_3 has been reported in the thermolysis of pentaerythirtyltetraammonium nitrate[8] and 1,2,3-triaminoguanidinium nitrate.[48] It is also evident that a part of each salt also undergoes sublimation, which was confirmed by heating each salt at an appropriate temperature.

C−N bond fission also takes place, liberating NH_3 (confirmed by chemical analysis), which is the accepted product of the decomposition of PDADP since the O/H ratio of all perchlorate salts is <1. It is reported[49,50] that salts with O/H < 1 have been found to release NH_3(g), while those with O/H ≥ 1 do not. Nambiar et. al[3] have also reported the evolution of NH_3 as a dissociation product of methylammonium perchlorate.

Conclusions

The thermolysis of PDADP seems to involve proton transfer from the anilinium ion to the ClO_4^- ion as the primary rate-controlling step. At higher temperature, interaction between phenylenediamine (fuel part) and the ClO_4^- ion (oxidizer) formed leads to an explosion. A part of the perchlorate may undergo sublimation.

Supporting Information Available: Additional experimental procedures. This material is available free of charge via the Internet at http://pubs.acs.org.

References and Notes

(1) Kennan, A. G.; Siegmund, R. F. *J. Solid State Chem.* **1972**, *4*, 362.
(2) Singh, G.; Kapoor, I. P. S. *J. Energ. Mater.* **1993**, *11*, 293.
(3) Nambiar, R. R.; Pai Verneker, V. R.; Jain, S. R. *J. Therm. Anal.* **1975**, *7*, 15.
(4) Nambiar, R. R.; Pai Verneker, V. R.; Jain, S. R. *J. Therm. Anal.* **1975**, *8*, 587.
(5) Udupa, M. R. *Thermochim. Acta* **1980**, *42*, 383.
(6) Udupa, M. R. *Thermochim. Acta* **1983**, *71*, 219.
(7) Russel, T. P.; Brill, T. B. *Propellants, Explos., Pyrotech.* **1990**, *15*, 123.
(8) Russel, T. P.; Brill, T. B. *Propellants, Explos., Pyrotech.* **1990**, *15*, 77.
(9) Chem, R.; Russel, T. P.; Rheingold, A. L.; Brill, T. B. *J. Crystallogr. Spectrosc. Res.* **1991**, *21*, 167.
(10) Russel, T. P.; Brill, T. B. *Propellants, Explos., Pyrotech.* **1990**, *15*, 281.
(11) Russel, T. P.; Brill, T. B. *Propellants, Explos., Pyrotech.* **1990**, *15*, 27.
(12) Russel, T. P.; Brill, T. B. *Combust. Flame* **1989**, *76*, 393.
(13) Singh, G.; Kapoor, I. P. S. *J. Phys. Chem.* **1992**, *96*, 1215.
(14) Singh, G.; Kapoor, I. P. S.; Mannan, S. M. *J. Therm. Anal.* **1996**, *46*, 1751.
(15) Singh, G.; Kapoor, I. P. S.; Mannan, S. M. *J. Energ. Mater.* **1995**, *13*, 141.
(16) Singh, G.; Kapoor, I. P. S. Jacob, S. *J. Sci. Ind. Res.* **2000**, *59*, 575.
(17) Singh, G.; Kapoor, I. P. S.; Jacob, S. *Indian J. Eng. Mater. Sci.* **1998**, *5*, 140.
(18) Kapoor, I. P. S.; Srivastava, P.; Singh, G. *J. Hazard Mater.* **2007**, in press.
(19) Basset, J.; Denny, R. C.; Jaffey, G. H.; Manehan, J. *Vogel's Text Book of Quantitative Inorganic Analysis*, 4th ed; Longmavnn: London 1985; p 497.
(20) Hooft, R. *COLLECT Data Collection Software*; Nonius B V: Delft, The Netherlands, 1998.
(21) Otwinowski, Z.; Minor, W. *Methods Enzymol.* **1997**, *276*, 307.
(22) Sheldrick, G. M. *Acta Crystallogr., Sect. A* **1990**, *46*, 467.
(23) Sheldrick, G. M. *SHELXTL-NT*, version 6.12, reference manual; University of Göttingen: Göttingen, Germany, 2000.
(24) Klaus, B. *DIAMOND*, version 1.2c; University of Bonn: Bonn, Germany, 1999.
(25) Singh, G.; Singh, R. R. *Res. Ind* **1978**, 23, 92.
(26) Singh, G.;Vasudeva, S. K.; Kapoor, I. P. S. *Indian J. Technol.* **1991**, *29*, 589.
(27) Semenov, N. *Chemical Kinetics and Chain Reactions*; Clarendon Press: Oxford, U.K., 1935; Chapter 18.
(28) Freeman, E. S.; Gordon, S. *J. Phys. Chem.* **1956**, *60*, 867.

(29) Zinn, J.; Rogers, R. N. *J. Phys. Chem.* **1962**, *66*, 2646.
(30) Singh, G.; Singh, R. R.; Rai, A. P.; Kapoor, I. P. S. *J. Therm. Anal.* **1990**, *36*, 2539.
(31) Martin, A. R.; Yallop, H. J. *Trans. Faraday Soc.* **1958**, *54*, 257.
(32) Rothstein, L. R.; Peterson, R. *Propellants, Explos., Pyrotech.* **1979**, *4*, 56.
(33) Brown, M. E.; Dollimore, D.; Galway, A. K. *Comprehensive Chemical Kinetics*; Elsevier: Amsterdam, The Netherlands, 1960; Vol. 22.
(34) Vyazovkin, S. V. *Int. J. Chem. Kinetics* **1996**, *28*, 95.
(35) Singh, G.; Kapoor, I. P. S. *J. Chem. Soc., Perkin Trans. 2* **1989**, 2155.
(36) Singh, G.; Kapoor, I. P. S.; Jain, M. *J. Chem. Soc., Perkin Trans. 2* **1993**, 1521.
(37) Singh, G.; Kapoor, I. P. S.; Jain, M. *Indian J. Chem., Sect. B* **1996**, *35*, 369.
(38) Singh, G.; Kapoor, I. P. S.; Jain, M. *Thermochim. Acta* **1997**, *1*, 3166.
(39) Singh, G.; Kapoor, I. P. S.; Singh, J. *Indian J. Eng. Mater. Sci.* **1998**, *5*, 300.
(40) Singh, G.; Kapoor, I. P. S. *Combust. Flame* **1993**, *92*, 283.
(41) Singh, G.; Kapoor, I. P. S.; Mannan, S. M.; Agrawal, J. P. *Combust. Flame* **1994**, *97*, 355.
(42) Singh, G.; Kapoor, I. P. S.; Mannan, S. M. *Thermochim. Acta* **1995**, *262*, 117.
(43) Zsako, J.; Artz, H. E. *J. Therm. Anal.* **1974**, *6*, 651.
(44) Dollimors, D.; Roelgers, P. F. *Thermochim. Acta* **1979**, *30*, 273.
(45) Cremer, E. Z. *Adv. Catal.* **1955**, *7*, 75.
(46) Garn, P. D. *Thermochim. Acta* **1979**, *28*, 185.
(47) Burnham, A. K.; Dinh, L. N. *J. Therm. Anal. Calorim.* **2007**, *89*, 479.
(48) Russell, T. P.; Brill, T. B. *Propellants, Explos., Pyrotech.* **1990**, *15*, 66.
(49) Oyumi, Y.; Brill, T. B. *J. Phys. Chem.* **1985**, *89*, 4325.
(50) Oyumi, Y.; Brill, T. B. *J. Phys. Chem.* **1987**, *91*, 3657.